

RESEARCH ARTICLE

Open Access



# Porous space — biomimetic of tafoni in computational design

Wei Ye<sup>1\*</sup> , Shuhua Chen<sup>1</sup>, Xiayu Zhao<sup>1</sup> and Weiguo Xu<sup>2</sup>

## Abstract

Porous urban spaces not only improve interactions, but also increase natural ventilation. Weathered rocks are where porous spaces exist in nature. This paper investigates the biomimicry of tafoni, a type of weathered rock that contains pores of varying sizes. The formation of tafoni inspires architectural design, but its complex shape makes manual modeling challenging. The objective of studying the biomimetics of tafoni is to apply its benefits to design applications. Using biomimetic techniques, computation algorithms for tafoni morphogenesis are developed. This paper investigates the inherent characteristics of tafoni and reclassifies them based on architectural geometric elements. It then describes the reclassified tafoni and explains the formation process. This paper develops a 3D evolutionary algorithm and a 2.5D descriptive algorithm based on diagrams. After a comparison, the 2.5D algorithm is chosen because it is more controllable and operable for computational design. This paper also conducts experiments on the results obtained by the 2.5D algorithm to demonstrate its adaptability and architectural design application potential, as well as its application schemes in various design disciplines, including urban planning, architectural design, and landscape design. This paper proposes an algorithm that can be utilized in various fields of computational design. It is computationally efficient while retaining its biological form.

**Keywords:** Tafoni, Biomimetic, Computational design, Parametric morphology, Generative design, Porous space

## 1 Introduction

The evolution of architectural design and building technology has resulted in a rapid transformation of urban areas. Increasing urban interaction has become the top priority for urban development scholars in the 21st century. The desire for a "porous" city is indicated by the need for the transformation of the city to create space for efficient and effective interaction (Thierstein, 2018).

Porosity is a descriptive and analytic metaphor applicable to the category of urban planning agendas (Wolfrum, 2018a). Open porosity is technically defined as interconnected voids that allow gases and liquids to freely pass through a material, which has significant implications for cities because open porous materials can absorb various substances (Harnack, 2018). Porosity is a spatial feature

that popularized free connections, including the interpenetration and superposition of spaces, the integration and overlap of multi-level spaces, and the fuzzy spaces of interaction, etc. (Wolfrum, 2018b; Zohrer, 2018). The porous city concept eschews simple binary solutions; rather, it seeks to create urban space as an open system with a specific architectural design that can accommodate future change. In his political position, Stavrides (2006) asserts, "Urban pores in principle connect and establish opportunities for exchange and communication, eliminating thus space-bound privileges." Wolfrum (2018b) contends that the porous city has become an urban agenda to liberate urban culture on this basis. If frontiers are deemed to be an important aspect of urban planning, then the porous city should be prized, since high porosity maximizes the city's frontiers (Ursprung, 2018).

MVRDV presented the "Porous City" exhibition in 2012, showcasing their research on skyscraper design and the potential of porosity as a strategy for urban

\*Correspondence: yew21@mails.tsinghua.edu.cn

<sup>1</sup> Tsinghua Shenzhen International Graduate School, Shenzhen 518055, China  
Full list of author information is available at the end of the article

density. It transformed the city into a vertical high-porosity tower with parks, public spaces, and a mixed urban design (Maas, 2012). The porous school design of the Visual Arts Building at the University of Iowa was created by Steven Holl Architects. The building is composed of vertical porous volumes, and the fluid spaces are designed to facilitate maximum interaction between the school's various departments. Simultaneously, natural light and ventilation enter the building's core through the "light center" (Steven Holl Architects, 2016).

In addition to enhancing interactions, porous space can effectively affect urban environments' natural ventilation (Yuan, 2012). Natural ventilation is an effective architectural strategy that not only decreases building energy consumption (Etheridge, 2012), but also increases user satisfaction (Allard & Santamouris, 1998). Hirano (2006) investigated the effect of component-scale voids on cooling load reduction and the effect of building-scale voids on CO<sub>2</sub> emission reduction in porous residential buildings. It was discovered that building-scale voids are highly efficient at reducing cooling load. Saadatjoo et al. (2017) examined the impact of porosity distribution patterns on the performance of natural ventilation in buildings. In comparison to solid models, porous residential blocks improved natural ventilation performance by up to 64%, according to the findings. This research contributes to a greater comprehension of flow patterns in buildings with various porosity distribution patterns.

In the mid-1920s, Walter Benjamin and Asja Lacin proposed porosity as a metaphor for space, life, and society in Naples, which reminded them of grottos and caves in rocks: "As porous as this stone is the architecture" (Benjamin & Lacin, 1925). Natural sedimentary stones that have undergone a lengthy period of natural weathering are considered to have a porous structure (Doehne, 2010). While the theory of biomimetic design states that the form of nature can inspire architectural design (Menges, 2012), we question whether the morphology of naturally weathered rocks can serve as the spatial prototype for pore city.

In this paper, tafoni, a type of weathered rock containing pores of varying sizes, is chosen for investigation. The term tafoni has been adopted to describe cavities in rock faces (Penck, 1894) and they are typically formed by marine abrasion, wind corrosion, and mechanical weathering (Paradise, 2015). Paradise (2015) defined tafoni as "lace-like, honeycomb, bowl, or pan-shaped cavities occurring in a variety of rock types and locations that show a commonly unique assemblage and morphology." Tafoni contains porous spaces of varying sizes. Its internal structure is formed by the spaces between the interior and exterior, with smooth, curved surface connections between the spaces (Inkpen & Hall, 2019).

Biomimicry offers a novel approach to applying nature's solutions to human problems (Khosromanesh & Asefa, 2019). The organizational, structural, and functional principles of natural objects inform biomimetic design (Menges, 2012). This paper aims to study the biomimetics of tafoni and implement its benefits in architecture, based on the premise that the porous space of tafoni can provide favorable conditions for architecture, such as sufficient interaction space and natural ventilation. It is possible to implement biomimetic design processes in architecture using computational design. It is an exploratory method distinct from engineering that utilizes natural analogy algorithms (Menges, 2012). Under the direction of the computational design program, the generation and evolution of form can be conducted under regulated conditions. It is possible to generate results that adhere to the same program logic but respond differently to external forces, environments, and functional requirements (Menges, 2012).

This paper concludes by applying the computational biomimetic design method to the development of tafoni generation algorithms, evaluating the applicability of the algorithms for computational design, and presenting the results and application schemes for the algorithm.

## 2 Methodology

The biomimetic computational design methodology is based on the computation algorithm of morphogenesis. The term "morphogenesis" refers to the developmental progression of biological systems from birth to maturity, as well as their morphological evolution (Menges, 2012). Various methods have been used in the past to investigate the morphogenesis of a natural organism, including abstract diagram analysis (Xu & Li, 2018), botanic theoretical research (Khosromanesh and Asefi (2019), and computational simulation (Feng et al., 2021).

In previous studies, Xu et al., (2018) used symbiotic phyllotaxy as an illustration, analyzed the biological mechanism using an abstract graphic, developed the generation algorithm, and proposed architectural design applications. Khosromanesh and Asefi (2019) conducted extensive research in the field of botany before employing parametric design tools to transform the solutions in botany into the mechanism for an environmentally friendly building envelope. Based on the steady-state effect of Taihu stone, Z. Feng et al., (2021) developed a generative design method that combines the techniques of computational fluid dynamics (CFD) simulation and bidirectional progressive structural optimization (BESO).

The biomimetic design processes in architecture are morphogenetic and evolutionary, according to Menges (2012). Four methods are presented for the development of the generative algorithm: feature-based,

constraint-based, process-based, and feedback-based. While the form of tafoni serves as inspiration for the form-finding process of porous spaces, the methodology of this paper is "feature-based."

Botany, biology, geology, and other disciplines have excavated the characteristics of natural forms from their respective vantage points, but is there an architectural way to describe natural form characteristics? Imhof (2013) proposed that natural principles must be abstracted when studying natural patterns in bionics. Gruber and Imhof (2017) obtained the evolution map of slime mold growth by photographing the growth of natural slime molds and applying computational processing to simplify the images. In their 2018 book "Digital Diagrams from BIO-Form for Architectural Design," Xu and Li describe a method of using abstract diagrams to geometricize "features" in order to achieve parametric generation. Their diagrams are obtained through observation and simplification through abstraction, and they can directly describe the geometric characteristics.

This paper divides "feature-based" biomimicry into two categories: description and evolution. The objective of the former is to directly describe the characteristics based on observation, while the objective of the latter is to explain the internal causes of its formation. "Description" emphasizes external shapes, which is more conducive to form generation in computational design; "Evolution" emphasizes internal reasoning, which is more conducive to simulating the dynamic shape changes that occur in

nature. The research process entails several steps. First, tafoni is selected for its abundance of porous spaces. This study reclassifies the natural form and employs diagrams to explain and describe it. Then, based on the generation rules of the description and evolution diagrams, two algorithms are deduced. This paper selects the algorithm that is more feasible for computational design by comparing the two algorithms. Based on the various input variables, the chosen algorithm is then used to generate a series of forms. The algorithm is then experimentally evaluated and architecturally prototyped. (Fig. 1).

### 3 Biomimetic algorithms

This paper reclassifies the natural form of tafoni in order to diagrammatically evaluate them. The study and classification of weathered rocks began as early as the 19th century. The first honeycomb cavities with a diameter greater than 0.5 m were referred to as tafoni (Penck, 1894). Paradise defined tafoni as "lace-like, honeycomb, bowl, or pan-shaped cavities occurring in a variety of rock types and locations that show a commonly unique assemblage and morphology." (Paradise, 2015). Previous authors have proposed classification methods such as alveoli, stone lace, honeycombing, caverns, and pitting when studying weathered rocks, so far none of them have been able to provide a shared terminology of classification and morphological distinction (Groom et al., 2015). Tafoni can be classified differently depending on one's perspective. This paper focuses on extracting the

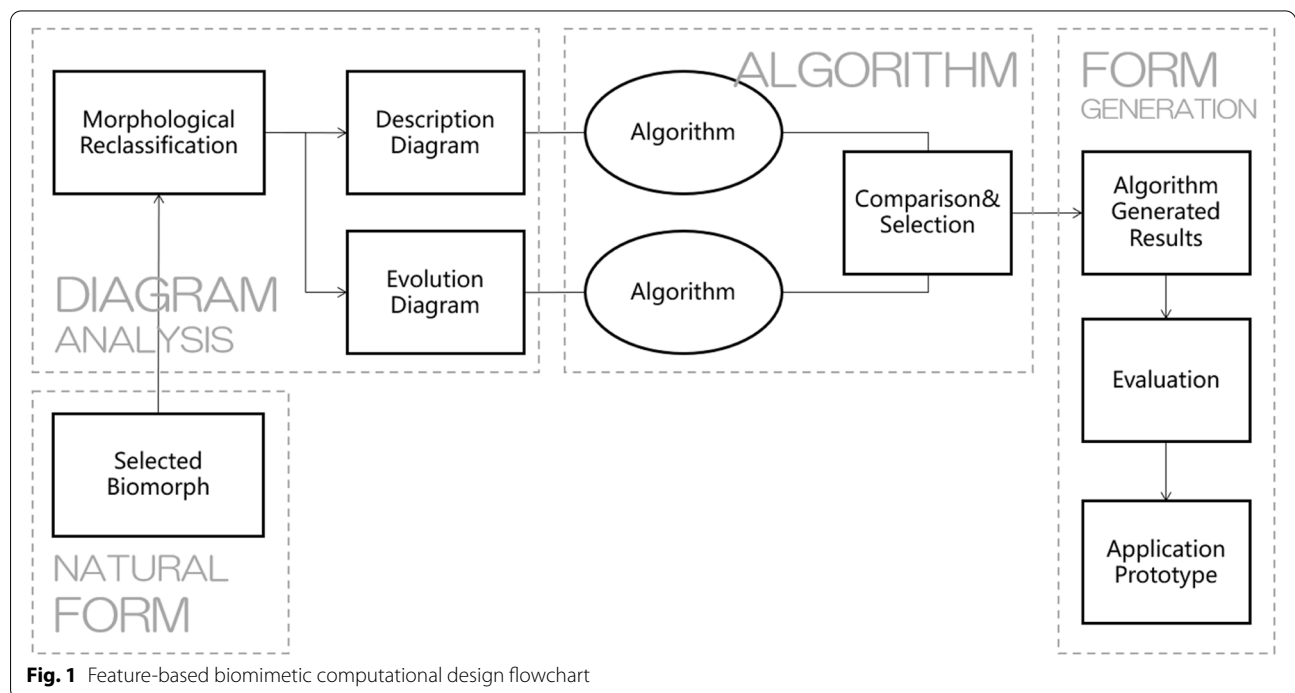


Fig. 1 Feature-based biomimetic computational design flowchart

morphological characteristics of tafoni and incorporating them into architectural design. Point, line, and surface are the fundamental visual elements for expressing space and entity, as well as the fundamental compositional elements of architectural plans. This study classifies the morphology of tafoni into three categories: point-based, plane-based, and line-based.

**3.1 Description**

The description of three types of tafoni were separately developed. The three classified natural form and corresponding description diagrams are shown in Fig. 2 below.

**3.1.1 Point-based tafoni**

Point-based tafoni, also known as honeycombs, has irregularly concave holes of varying sizes and organic shapes, as well as an inconsistent concave surface depth. Over time, concave holes become larger and deeper in the form of cavities, while the non-concave portion develops a ribbed appearance. In some instances, the space between adjacent pores vanishes following depression, leaving only the upper portion of the distinct rib. Voronoi is a 2D computational algorithm that has been utilized in the past to mimic point-based tafoni (Doe, 2011).

**3.1.2 Plane-based tafoni**

Plane-based tafoni has been exposed to the upward wind force generated by the local thermal cycle, blowing and abrading the weathering cavities with hook-like sides, concave in the middle and lower portions, rounded and smooth inner walls, and protruding like a cap tongue at the top.

**3.1.3 Line-based tafoni**

Line-based tafoni has irregular holes of varying sizes that are fused together, forming grooves where holes meet. The hole has varying lengths, thickness, bifurcation, and irregularly curved, strip-like grooves, and the grooves' depth is not uniform. The rib segment transforms into a continuous line.

**3.2 Evolution**

This section first reviews the natural causes of morphogenesis sequences, then creates evolution diagrams, and then converts the diagrams into computation algorithms.

**3.2.1 Weathering process**

Earlier research indicates that tafoni were formed in various types of bedrock, most commonly granitic

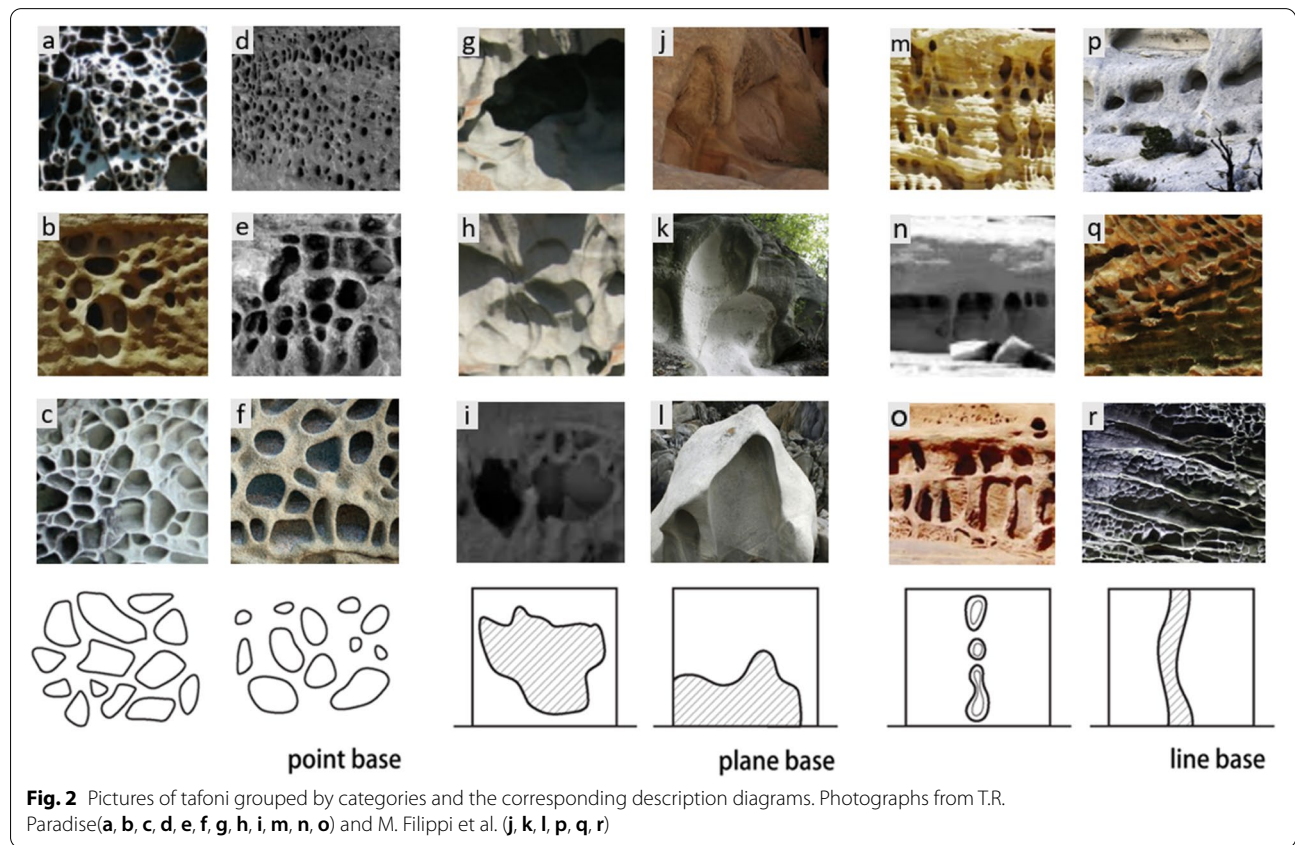


**Fig. 2** Pictures of tafoni grouped by categories and the corresponding description diagrams. Photographs from T.R. Paradise(a, b, c, d, e, f, g, h, i, m, n, o) and M. Filippi et al. (j, k, l, p, q, r)

rocks (Penck, 1894). Granitic weathering cavities are the result of various types of weathering and are closely associated with the granular structure, homogeneity, low permeability, and ease of disintegration of granites (Li et al., 2003). Burridge et al. proposed a model for the formation of craters caused by corrosive gases that can be compared to the process of weathering: each solid site is assigned an intensity value. If a corrosive particle occupies a site close to the surface and its next randomly selected step will bring it to the surface, there is a chance that the particle will degrade (Burridge & Inkpen, 2015). Microclimatic changes, salt weathering, and valley wind erosion are the primary factors that control and influence tafoni development as a whole (Huang & Wang, 2017). Valley wind erosion is a form of physical weathering, whereas salt weathering is a form of chemical weathering. Separate simulations of the physical and chemical weathering processes were conducted in this study.

Given that the bedrock of tafoni is generally granular in structure (Penck, 1894) and homogeneous (Li et al., 2003), this study chose to simulate the weathering process of tafoni using Orthogonal 3D point cloud.

### 3.2.2 Physical weathering

Physical weathering is brought about by valley wind erosion (Huang & Wang, 2017). It is the identical procedure for points, lines, and surfaces. The establishment of an iterative mathematical model of physical weathering. The study categorizes the forces acting on the 3D point cloud as interparticle force, wind force, and gravity. In this instance, the combined force on each point is calculated. Under the influence of an external force (wind force), the points in the point cloud with the smallest combined force are eliminated after each iteration. The wind vector value varies at random during each iteration. Iteration will continue until all points are eliminated. This process simulates the actual physical weathering process. The particle force analysis is shown in Fig. 3.

The plausibility of the physical weathering forces discussed in this paragraph has been verified and incorporated into the ESO and BESO algorithms, and the advantages of the optimized structure are maintained by removing ineffective or inefficient materials (Huang et al., 2007).

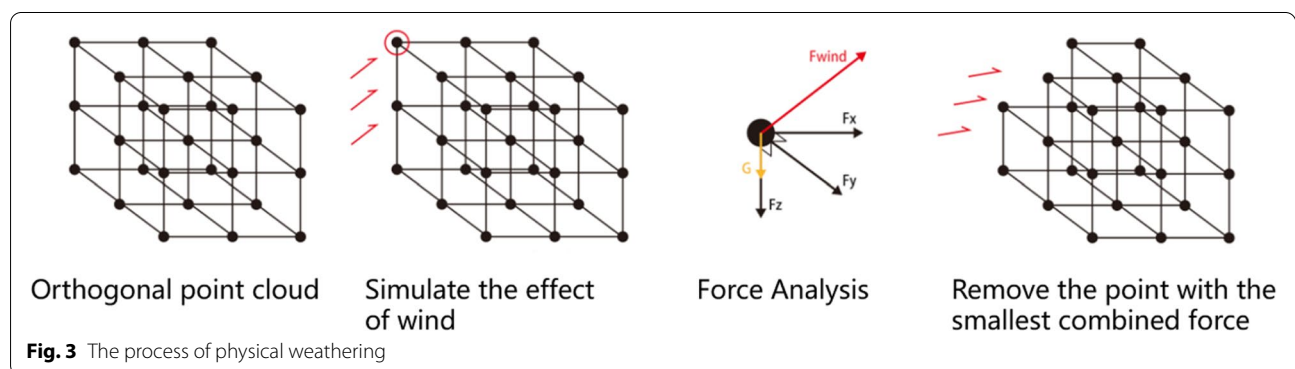
### 3.2.3 Chemical weathering

Chemical weathering rates were found to be related to lithology, microfracture, alteration, and cementation in Brandmeier’s study (Brandmeier et al., 2011), with alteration and cementation constituting chemical weathering. Consequently, our simulations concentrate on these two processes. A mathematical model of chemical weathering is constructed primarily on the basis of the two steps of chemical weathering: the decay of internal particles due to changes in humidity and the amplification of external particles due to gelation (Huinink & Kopinga, 2004). The two actions correspond to modification and cementation. As shown in Fig. 4, the processes of the three types vary within these two steps.

Based on the formation process analysis, we then developed generation rule models for the chemical weathering of three types of tafoni.

The initial input for point-based tafoni is the original mesh, followed by the generation of the orthogonal point cloud within the original mesh and the assignment of a value  $x$  to each point. When  $x$  is equal to or less than zero, the point is removed. Secondly, the selected points from the point cloud, which represents particle loss processes, are reduced. Thirdly, according to the two steps of chemical weathering, the calculation of two evolution rules is carried out:

- (i) The values of the neighboring points  $A$  in the vanishing particles decay.
- (ii) The values of the surface layer(exposed) points  $S$  increase.



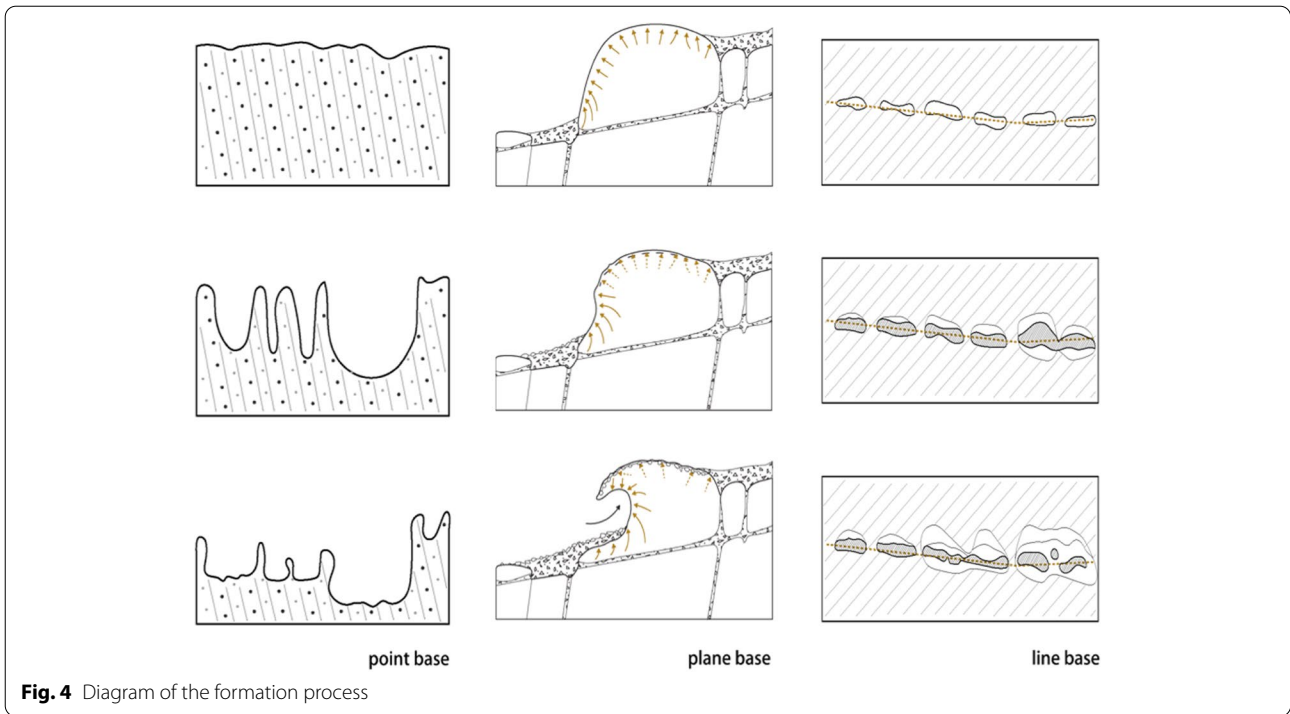


**Fig. 4** Diagram of the formation process

**For point A,**

$$x_a = x - N, \tag{3.1}$$

**For point S,**

$$x_s = x + \alpha N (0 < \alpha < 1), \tag{3.2}$$

**For a point X in point cloud,**

if  $x < 0$ , remove point X from point cloud,

( $N$  is the decay integer constant,  $\alpha$  is the enhancement ratio constant).

The chemical weathering process for plane-based tafoni is similar to that of point-based tafoni. Due to the large surface area of each cavity of the faceted weathering cavity, the temperature and humidity at different locations on its surface also vary (Matsukura & Tanaka, 2000), and the different temperatures and humidity exert a greater influence on the chemical weathering. The majority of chemical weathering occurs on the rock's more obscure, slower-drying surfaces. The upper portion of the tafoni is not directly exposed to sunlight and has a much slower drying rate than the lower portion; therefore, the weathering is more pronounced. Consequently, compared with the point-like evolution rule (i) and rule (ii), rule (iii) is added:

(iii) Decay degree of upper points  $a_1 >$  lateral points  $a_2 >$  lower points  $a_3$

**For point  $a_1$  point  $a_2$  point  $a_3$ ,**

$$x_{a1} = x - N, \tag{3.3}$$

$$x_{a2} = x - \beta N, \tag{3.4}$$

$$x_{a3} = x - \gamma N (0 < \gamma < \beta < 1), \tag{3.5}$$

**For point S,**

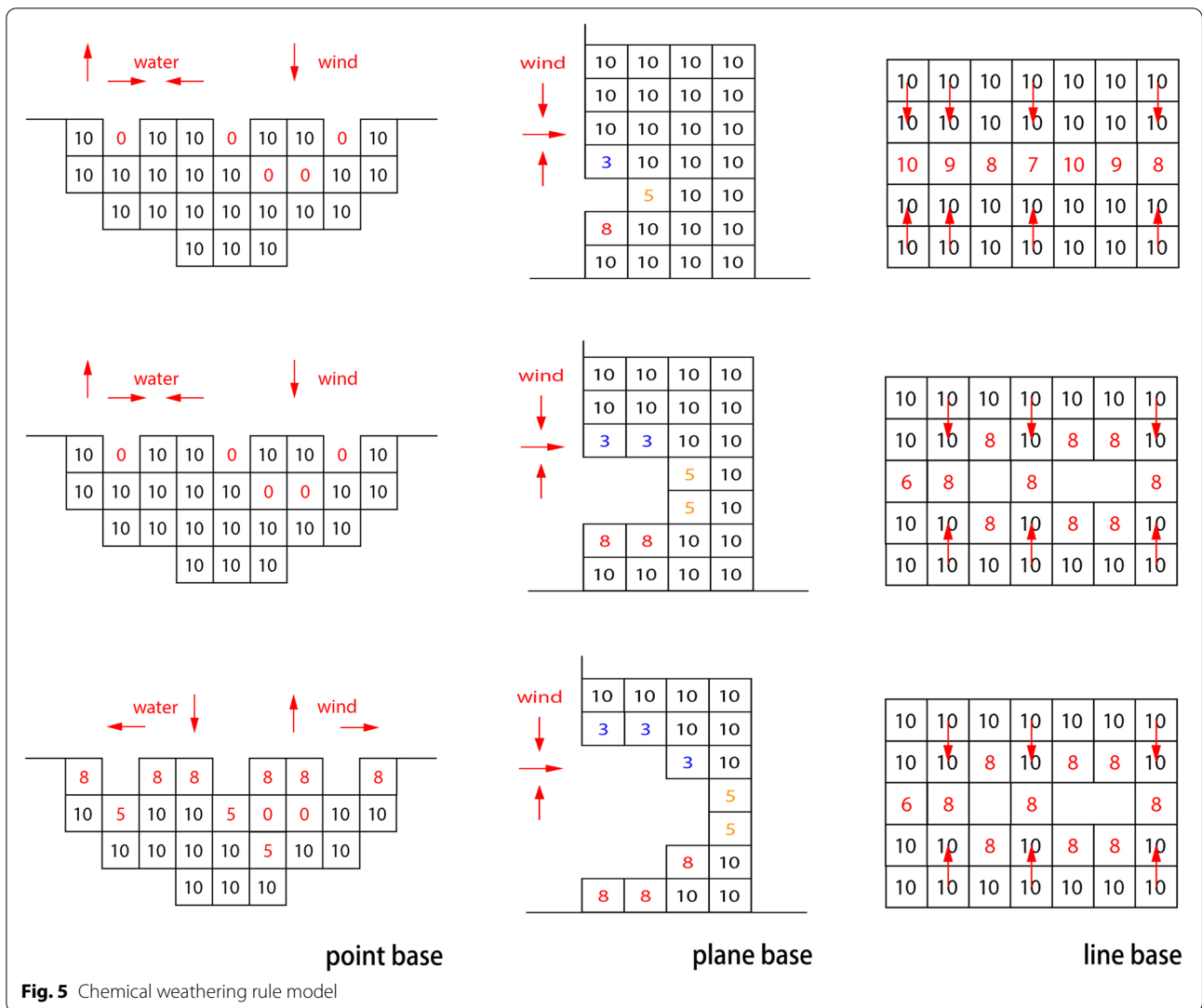
$$x_s = x + \alpha N (0 < \alpha < 1), \tag{3.6}$$

**For a point X in point cloud,**

if  $x < 0$ , remove point X from point cloud,

( $N$  is the decay integer constant,  $\beta$  and  $\gamma$  is the decay ratio constant,  $\alpha$  is the enhancement ratio constant).

Due to stress, the chemical weathering process differs for line-based tafoni (Filippi et al., 2018). The linear type of weathering is affected by stress, with no decay occurring for particles with greater stress and decay occurring for particles with lower stress. Therefore, the linear chemical weathering process must extend a straight line across the surface of the point set in order to delete less



stressed points at random. After the evolution rule (i), we add rule (iv):

- (iv) When there is no connection point on both sides of a point, set the point and all the points on its z-axis (stress points) as non-attenuating points.

**Set the set of stress points as  $\delta$**   
**For point A,**

$$x_a = x - N, \tag{3.7}$$

**For a point X in point cloud,**

**if  $x < 0$  , remove point X from point cloud,**

**if  $x \in \delta$  , do not remove point X from point cloud.**

The generation rule models of the three types of tafoni are shown in Fig. 5. The constants used in calculation can be adjusted according to the specific weathered rock characteristics.

### 3.3 Evolutionary algorithm

The evolutionary algorithm combines physical and chemical weathering to more accurately simulate the natural weathering process of tafoni. After studying physical weathering and chemical weathering processes separately, it is clear that chemical weathering is primarily responsible for shaping the various forms of weathered rocks (point-based tafoni, line-based tafoni, and plane-based tafoni). In the simulation of physical weathering, the angle of the external wind changes continuously

over time due to the valley wind erosion process. Consequently, the role of physical weathering in softening the cavities is more likely. The physical weathering process is simplified as a rock surface softening process in order to reduce the effects of physical weathering in the mixture. *Isosurface* is a smooth surface through all points between voxels, and the algorithm is simple to implement, so in this study, the *isosurface* algorithm is used to simulate the physical weathering effect. The process of combining chemical and physical weathering involves calculating the chemical weathering for the point cloud and then simulating the physical weathering using *isosurface*. The final simulation algorithm flowchart is shown in Fig. 6. The results of the simulation for the three types of natural tafoni are shown in Fig. 7.

### 3.4 Descriptive algorithm

The above tafoni evolutionary algorithm is iteratively calculated to simulate the evolution of tafoni. Naturally, the process of weathering takes billions of years. Similarly, the evolutionary algorithm requires a significant amount of computational time for each iteration to calculate the value of each point in the point set. In contrast, the descriptive algorithm derives formulas directly from descriptive diagrams while incorporating



Fig. 7 Algorithm results comparing with natural form

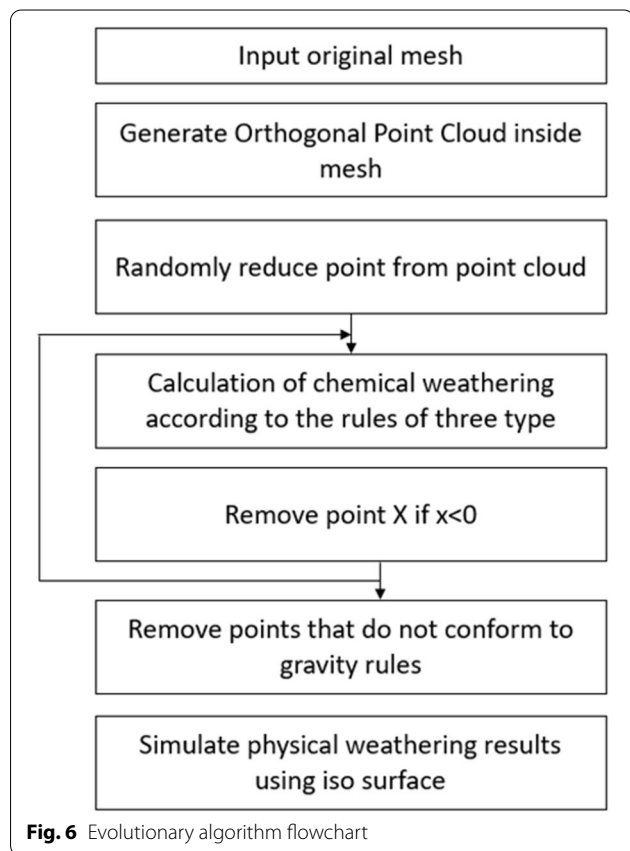


Fig. 6 Evolutionary algorithm flowchart

architectural design requirements. The descriptive algorithm computes two-dimensional points, which are then layered to form a point set. This paper describes the calculation as a 2.5D algorithm. (Figs. 8 and 9).

The 2.5D algorithm steps are as follows:

1. Input the initial volume mesh of the rock to be weathered;
2. Input the number of layers  $x$ . The number of layers can be converted into point cloud density parameters (because the point cloud for XYZ direction is equally spaced orthogonal point set, so the initial volume of the number of layers to convert the overall point density in the point cloud);
3. Generate the initial point cloud;
4. Generate 2D Voronoi control points by point type, line type, and surface type features, these control points are randomly generated by random number  $n$  control;
5. Generate the control Voronoi polygons and extract the polygons representing point type, line type, and surface type respectively;
6. The three corresponding polygons are divided, rounded, offset, and other operations;
7. Merge into the final set of closed curves;



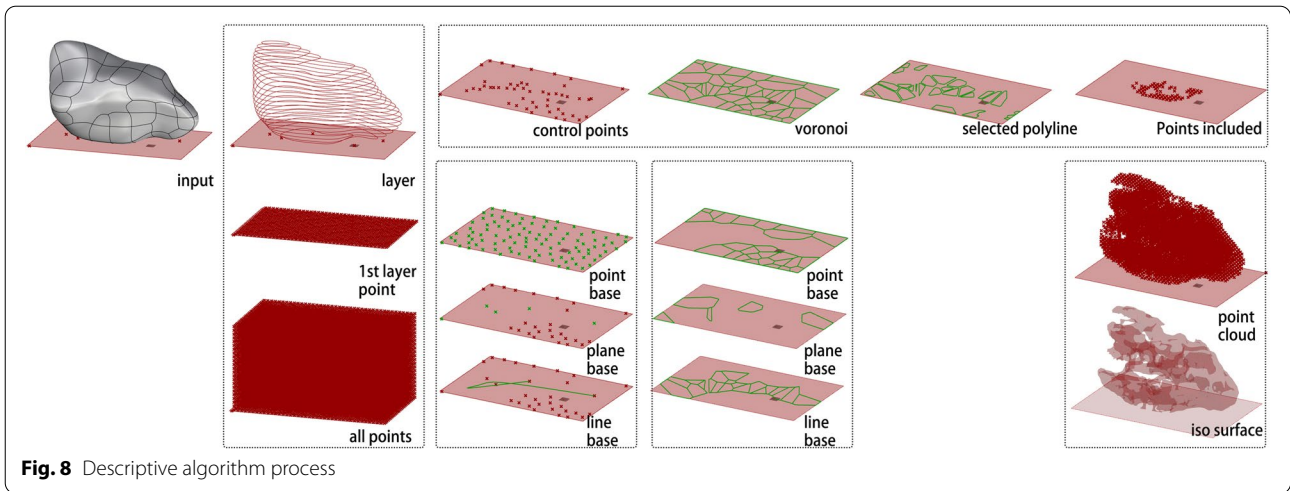


**Fig. 8** Descriptive algorithm process

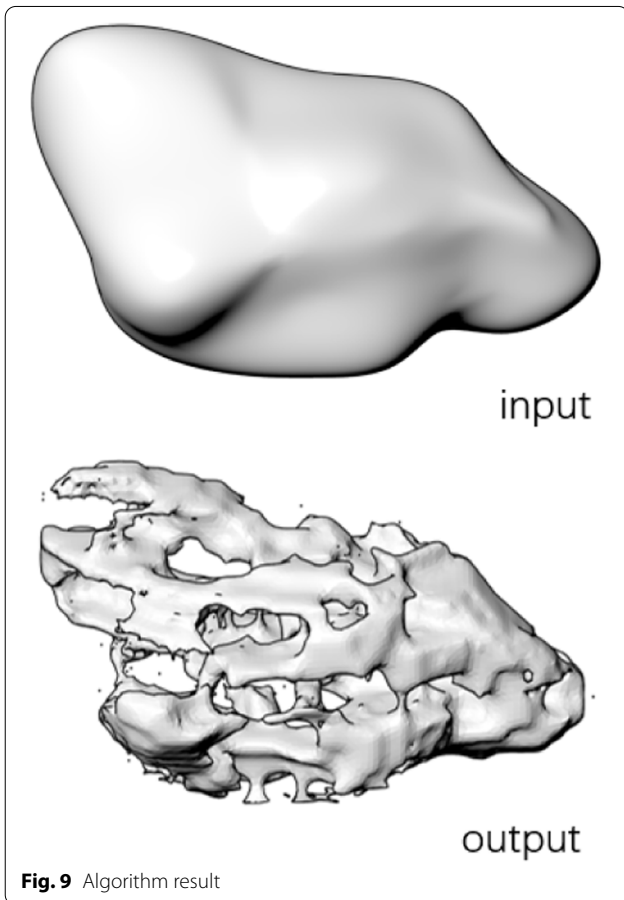


**Fig. 9** Algorithm result

8. Calculate whether the point cloud and the curve set are contained or not, and remove the points contained by the curve set;
9. Loop  $x$  times to get the points kept in each layer, these points form the final point set. In the calcula-

tion, it is found that the more the number of layers, the more laminar the generated form is. In order to eliminate the laminarization, a formula is experimentally derived that, let when the number of layers is  $x$ , for a random number  $n$ , every  $(x-7) / 7$  cycles,  $n = n + 1$ ,

$$n = n + \left[ \frac{x-7}{7} \right]; \tag{3.8}$$

10. Use *Isosurface* to convert the points to mesh. The effective range of iso is calculated by comparing and setting the number of layers to  $x$  as follows,

$$effective\ range = \frac{3000}{x-53}. \tag{3.9}$$

### 3.5 Comparison

For the purpose of applying the algorithm to architectural design, it must be simplified and made more user-friendly. The evolutionary algorithm is calculated iteratively, step by step. It simulates not only the shape of tafoni, but also its evolution. However, it includes the process of calculating all points and assigning values to them one by one and then iteratively calculating them, which consumes a great deal of computing power and time. For the input mesh volume, when the calculated point cloud density  $\rho$  is low (the number of points in the point cloud is small), the algorithm can be easily calculated. However, when a high-precision calculation is required, the point cloud density increases and the computation time increases significantly; consequently, the algorithm is not suited for practical design applications. The descriptive algorithm, on the other hand, only simulates the shape of the natural form, but it is feasible for the design approach.

The computational time complexity of the 3D algorithm and the 2.5D algorithm is estimated. If, for the same input mesh whose volume is  $V$ , the internal orthogonal point cloud density is set to  $\rho$  ( $\rho > 1$ ), then the number of points to be calculated from the point cloud is  $N$ . The formula for  $N$  is as follows,

$$N = \rho V. \quad (3.10)$$

The evolutionary 3D algorithm must first assign a value to each point before progressively reducing them until they disappear. Each point must be computed using  $N$  points. The sum of  $N$  points is determined. It requires  $N^2$  steps to calculate through all points, followed by  $N$  steps to assign the value. The time complexity can be estimated as  $N^3$ , which is then converted into the formula calculated by while ignoring constraints. The time complexity  $O_1$  is as follows,

$$O_1(\rho) = \rho^3. \quad (3.11)$$

For the 2.5D algorithm, the number of points per layer is  $\sqrt[3]{N^2}$ , and the loop operation is  $\sqrt[3]{N}$  steps from the bottom loop to the end of the topmost layer. The time complexity can be estimated as  $N$ . Neglecting the constants, the time complexity  $O_2$  is as follows,

$$O_2(\rho) = \rho. \quad (3.12)$$

Comparing time complexity  $O_1$  and  $O_2$ , the 2.5D algorithm can greatly reduce the time complexity of the algorithm since  $\rho > 1$ .

Although the 3D algorithm is capable of simulating the weathering process, its computational complexity cannot be supported by a computer, and it is difficult to modify it according to the actual design conditions. The computational complexity of the 2.5D algorithm for simulating weathered rock is low, and it is simpler to adjust the generated shape by the proportion of line type, plane type, and point type according to different design conditions. Compared to Voronoi and ESO/BESO, it has richer continuous porous spaces and less computational time complexity.

## 4 Evaluation

In order to assess the feasibility of the proposed algorithm to computational design, evaluation experiments are conducted on the 2.5D algorithm results in this paper. For a more intuitive comparison, the subsequent experiments generate their results from the same input mesh.

### 4.1 Algorithm flexibility

The algorithm's flexibility is tested. The algorithm's embedded internal parameters can be modified. Using

this algorithm, a comparative study was conducted. Using the same mesh and distinct control variables, we obtained distinct outcomes. The controlled variables consist of the point cloud density within the mesh (input  $n$ ) and the random seed number for the algorithm (input *seed*).

#### 4.1.1 Input different point density

As depicted in Fig. 10, when the value of  $n$  and the density of points in the volume are greater, the more intricately carved the generated shape is, the lower the point density and the rougher the generated shape becomes. These six graphs in the upper portion of Fig. 10 illustrate the generated results of the algorithm with the same seed input and six different  $n$  values, from rough to fine.

#### 4.1.2 Input random seed values

As depicted in Fig. 10, when the input value  $n$  is fixed, different seed values may produce different results with similar characteristics. This demonstrates the flexibility of the results generated. By combining performance analysis with other form-influencing factors, it is possible to evaluate and select the results. The twelve graphs in the lower portion of Fig. 10 illustrate the algorithm's results when given the same input  $n$  and random *seed* value.

## 4.2 Architectural application feasibility

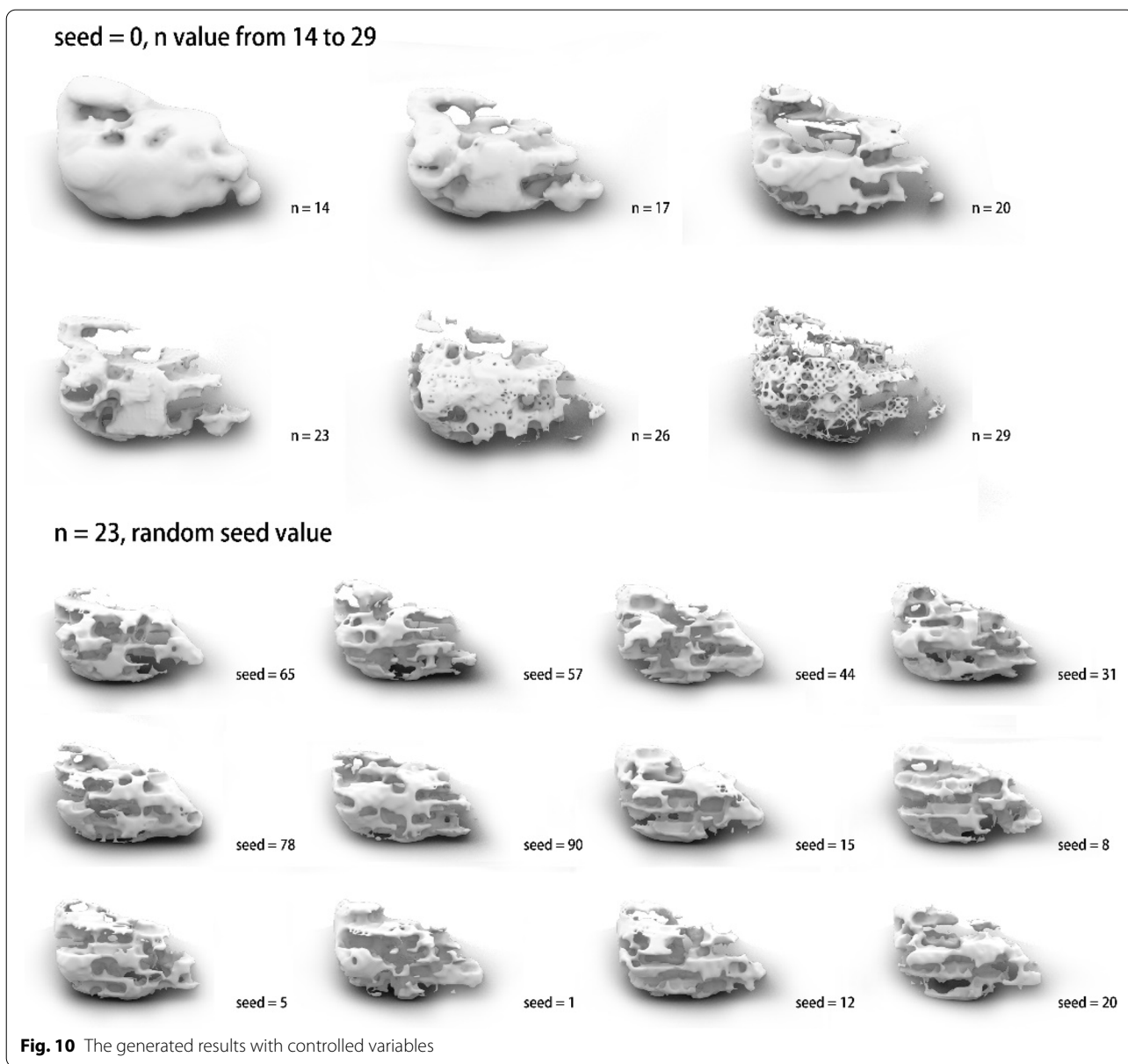
In order to use the generated results in architectural design, it is necessary, in addition to having a variety of architectural porous spaces, to assess the practicability of their use. Experiments were conducted on concavity, slope angle, and section shape richness. The results are shown in Fig. 11.

### 4.2.1 Concavity

The concavity is computed, and the results are depicted in the figure below. The result of the convex portion (colored blue) is greater than 0 for the entire shape, while the result of the concave portion (colored purple) is less than 0. According to the results, the concave portion of the mesh is roughly twice as large as the convex portion.

### 4.2.2 Mesh slop

Using the draft angle analysis, the slope of the result meshes was analyzed. Set a parameter of  $60^\circ$  based on the general slope of a building to determine if a portion of the mesh can be designed as a floor. A draft angle greater than the maximum value displays in blue. Between the maximum value and 0, a blue-green gradient is displayed.



A draft angle less than the minimum value displays in red. Between 0 and the lower value, a green–red gradient is displayed.

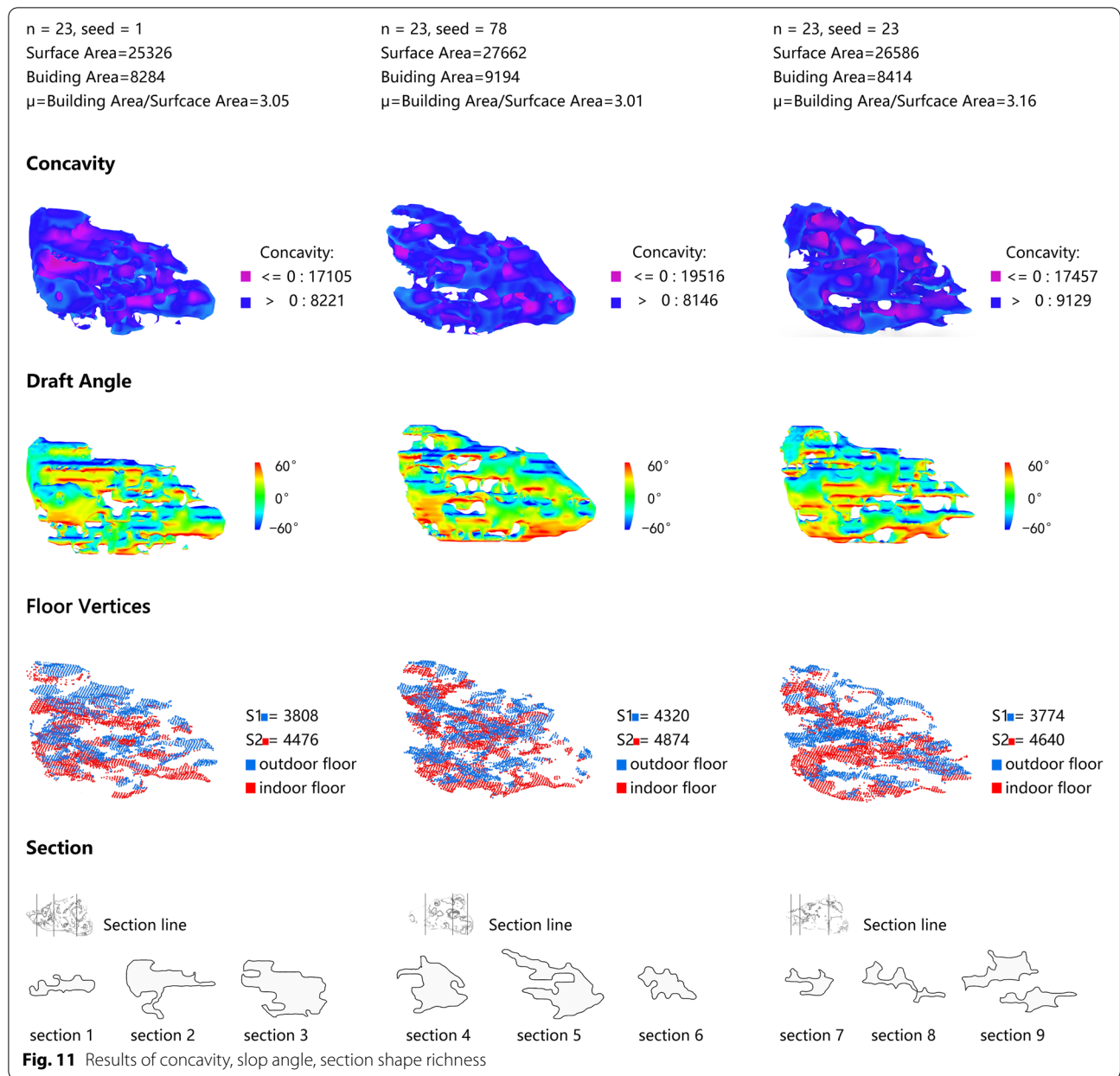
The mesh was then separated based on color. The mesh vertices of the blue and red color portions were extracted, and the number of mesh vertices of the blue and red portions as outdoor and indoor floor vertices was calculated. The ratio of total vertices to floor vertices was approximately 3.0~3.2, which can be extrapolated to estimate the ratio of a building’s surface area to its floor area.

#### 4.2.3 Section series

The sections of the resulting mesh are also calculated. As shown in Fig. 11, different activities can take place due to the richness of available spaces in the sections.

### 5 Application

This study demonstrates the application of the algorithm at three different design scales in order to achieve the purpose of applying the algorithm to computational design. In the application of biomimicry in architectural design, the form and structures of individual "organisms" are imitated, whereas in urban design, biomimicry is used



to imitate entire ecological systems (Uchiyama, 2020). On a scale of urban design, the biomimicry of tafoni provides designers with abundant associations. Due to the fact that the formation of tafoni is influenced by numerous external environmental parameters, they can be associated with social environmental factors, such as the flow of people, and used to aid in urban design. On a scale of architectural design, point, line, and plane correspond to private rooms, corridors, and public spaces, respectively. By applying the weathering algorithm to design, the embedded point, line, and plane types of tafoni can be used to generate urban space with various functions.

### 5.1 Urban design

The study presents an urban design scheme for Inujima, Japan. The scheme designs a weathered island one hundred years from now. Existing residential foundations, road foundations, and mine pits have weathered, resulting in point-based, linear-based, and plane-based weathering, respectively. The original site and the weathered result are shown in Fig. 12. Control points are established through existing elements, and the degree of weathering is controlled by layer based on functional requirements. A plot on the weathered island is chosen for further development.

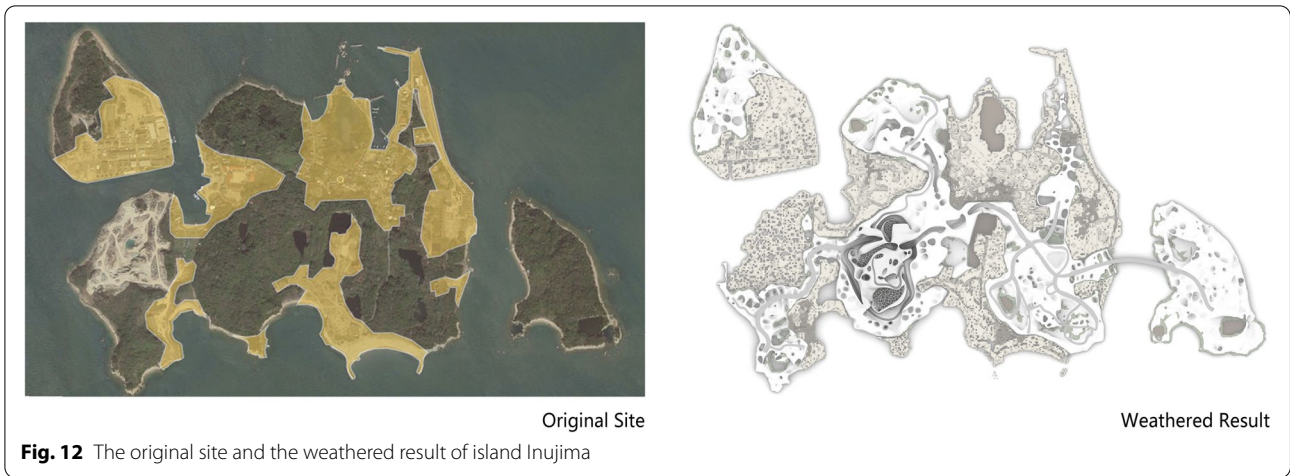


**Fig. 12** The original site and the weathered result of island Inujima

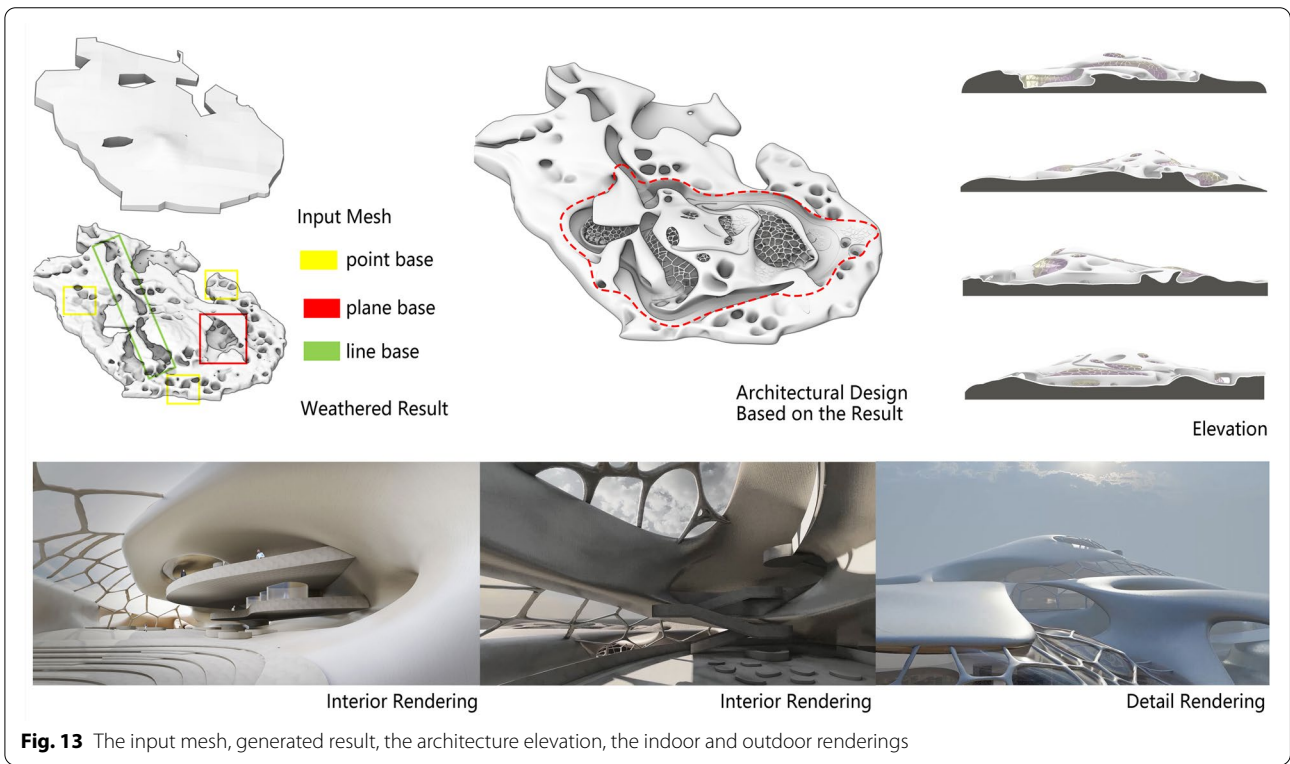


**Fig. 13** The input mesh, generated result, the architecture elevation, the indoor and outdoor renderings

### 5.2 Architecture design

Using the above-mentioned scenario, the study illustrates an architectural design scheme. The scheme begins by generating pore spaces in a rock, which are then designed as an office building. The point-based is intended for building rooms, the plane-based for public areas, and the line-based for transportation areas. The interior architectural spaces are further designed after the algorithm has been computed. Figure 13 depicts the input mesh,

generated result, architecture elevation, and indoor and outdoor renderings.

### 5.3 Pavilion design

In a traditional Chinese garden, weathered rocks are frequently used to enhance the garden's natural atmosphere. Applying the algorithm to architectural design, the study generated a Chinese garden pavilion using the developed algorithm. Not only does the complex porous space of the generated pavilion provide rich



**Fig. 14** The renderings and sections of an algorithm generated pavilion

light and shadow changes, but it also provides a rich experience for users to play within. In addition, its form is derived from nature and can be incorporated into the garden landscape, so this pavilion's artificial construction lacks any sense of artificiality. The renderings and the sections of the pavilion are shown in Fig. 14.

## 6 Conclusion and future work

In urban areas, porous spaces not only enhance interaction, but also increase natural ventilation.

This paper develops a 2.5D tafoni morphogenetic algorithm for computational architectural design using biomimetic techniques. Compared to previous research on 2D or 3D algorithms for generating weathered rock, this 2.5D algorithm can generate more porous spaces and requires less computational time. This algorithm can generate rich porous spaces and provide architectural form-finding inspiration by adjusting various parameters. The rich organic pore form of weathered rocks, the multi-directional penetration of horizontal and vertical space, and the flowing non-linear curved form reflect the application value and potential of this form, which will provide innumerable opportunities for future urban planning and architectural design.

This algorithm lays the groundwork for future studies on porous spaces. Future applications of the algorithm may include the generation of architectural design schemes with varying porosities. It is possible to compare their performance in order to confirm the natural ventilation efficiency of porous spaces. In addition, its construction can be considered during the algorithm development procedure.

### Acknowledgements

N/A

### Authors' contributions

The author(s) read and approved the final manuscript.

### Funding

N/A.

### Availability of data and materials

<https://github.com/WeiYe1904/tafoni-simulation-gh-script>

### Declarations

#### Competing interests

The authors declare that they have no known competing financial interests or personal relationships that could have appeared to influence the work reported in this paper.

### Author details

<sup>1</sup>Tsinghua Shenzhen International Graduate School, Shenzhen 518055, China.

<sup>2</sup>School of Architecture, Tsinghua University, Beijing 100084, China.

Received: 15 October 2022 Accepted: 21 December 2022

Published online: 30 December 2022

### References

- Allard, F., & Santamouris, M. (1998). *Natural Ventilation in Buildings: A Design Handbook*. James & James Ltd.
- Benjamin, W., & Lavis, A. (1925). Naples. In P. Demetz (Ed.), *Reflections, Essays, Aphorisms, Autobiographical Writings* (pp. 163–173). Harcourt Brace Jovanovich.
- Brandmeier, M., Kuhlemann, J., Krumrei, I., Kappler, A., & Kubik, P. W. (2011). New challenges for tafoni research. A new approach to understand processes and weathering rates. *Earth Surface Processes and Landforms*, 36(6), 839–852. <https://doi.org/10.1002/esp.2112>
- Burridge, J., & Inkpen, R. (2015). Formation and arrangement of pits by a corrosive gas. *Physical Review E*, 91(2), 022403. <https://doi.org/10.1103/PhysRevE.91.022403>
- Doe, N. A. (2011). The geometry of honeycomb weathering of sandstone. *Shale*, 26, 31–60.
- Doehne, E., & C. Price. (2010). *Stone Conservation: an overview of current research*. Los Angeles: The Getty Conservation Institute. H.; Toniolo, L.; and F. Cappitelli, Francesca, London: Archetype, 65–72.
- Etheridge, D. (2012). *Natural Ventilation of Buildings. Theory, Measurement and Design*. John Wiley & Sons Ltd.
- Feng, Z., Gu, P., Zheng, M., Yan, X., & Bao, D. W. (2021). Environmental Data-Driven Performance-Based Topological Optimisation for Morphology Evolution of Artificial Taihu Stone. *The International Conference on Computational Design and Robotic Fabrication* (pp. 117–128). Springer.
- Filippi, M., Bruthans, J., Rihošek, J., Slavík, M., Adamovič, J., & Mašin, D. (2018). Arcades: Products of stress-controlled and discontinuity-related weathering. *Earth-Science Reviews*, 180, 159–184. <https://doi.org/10.1016/j.earscirev.2018.03.012>

- Groom, K. M., Allen, C. D., Mol, L., Paradise, T. R., & Hall, K. (2015). Defining tafoni: Re-examining terminological ambiguity for cavernous rock decay phenomena. *Progress in Physical Geography*, 39(6), 775–793. <https://doi.org/10.1177/0309133315605037>
- Gruber, P., & Imhof, B. (2017). Patterns of growth—biomimetics and architectural design. *Buildings*, 7(2), 32.
- Harnack, M. (2018). Drifting Clouds: Porosity as a Paradigm. In S. Wolfrum (Ed.), *Porous City: From Metaphor to Urban Agenda* (pp. 38–41). Birkhäuser. <https://doi.org/10.1515/9783035615784-006>
- Hirano, T., Kato, S., Murakami, S., Ikaga, T., Shiraishi, Y., & Uehara, H. (2006). A study on a porous residential building model in hot and humid regions part 2—reducing the cooling load by component-scale voids and the CO2 emission reduction effect of the building model. *Building and Environment*, 41(1), 33–44. <https://doi.org/10.1016/j.buildenv.2005.01.016>
- Huang, R., & Wang, W. (2017). Microclimatic, chemical, and mineralogical evidence for tafoni weathering processes on the Miaowan Island, South China. *Journal of Asian Earth Sciences*, 134, 281–292. <https://doi.org/10.1016/j.jseaes.2016.11.023>
- Huang, X., Xie, Y. M., & Burry, M. C. (2007). Advantages of bi-directional evolutionary structural optimization (BESO) over evolutionary structural optimization (ESO). *Advances in Structural Engineering*, 10(6), 727–737. <https://doi.org/10.1260/136943307783571436>
- Huinink, H. P., Pel, L., & Kopinga, K. (2004). Simulating the growth of tafoni. *Earth Surface Processes and Landforms: The Journal of the British Geomorphological Research Group*, 29(10), 1225–1233. <https://doi.org/10.1002/esp.1087>
- Imhof, B., Gruber, P., Badura, J., & Lynn, G. (2013). *What is the Architect Doing in the Jungle?: Biomimetics*. Springer.
- Inkpen, R., & Hall, K. (2019). Universal Shapes? Analysis of the Shape of Antarctic Tafoni. *Geosciences*, 9(4), 154. <https://doi.org/10.3390/geosciences9040154>
- Khosromanesh, R., & Asefi, M. (2019). Form-finding mechanism derived from plant movement in response to environmental conditions for building envelopes. *Sustainable Cities and Society*, 51, 101782.
- Li, D. W., Cui, Z. J., Li, H. J., & Nan, L. (2003). Mechanism of granite weathering cave formation and environmental significance in northern China. *Journal of Nanjing University (natural Science Edition)*, 01, 120–128.
- Maas, W. (2012). *Porous city Lego towers*. Retrieved November 27, 2022, from <https://www.mrvd.nl/projects/179/porous-city-lego-towers>.
- Matsukura, Y., & Tanaka, Y. (2000). Effect of rock hardness and moisture content on tafoni weathering in the granite of Mount Doeg-Sung, Korea. *Geografiska Annaler: Series a, Physical Geography*, 82(1), 59–67. <https://doi.org/10.1111/j.0435-3676.2000.00112.x>
- Menges, A. (2012). Biomimetic design processes in architecture: Morphogenetic and evolutionary computational design. *Bioinspiration & Biomimetics*, 7(1), 015003.
- Paradise, T. R. (2015). Tafoni and Other Rock Basins. *Reference Module in Earth Systems and Environmental Sciences*, Elsevier. <https://doi.org/10.1016/B978-0-12-409548-9.09570-1>
- Penck, A. (1894). *Morphologie der erdoberfläche*. J. Engelhorn.
- Saadatjoo, P., Mahdavinnejad, M., & Zarkesh, A. (2019). Porosity rendering in high-performance architecture: wind-driven natural ventilation and porosity distribution patterns. *Armanshahr Archit Urban Dev*, 12(26), 73–87. <https://doi.org/10.22034/AAUD.2019.89057>
- Stavrides, S. (2006). Heterotopias and the experience of porous urban space. In *Loose Space* (pp. 174–192). Routledge. <https://www.taylorfrancis.com/chapters/edit/10.4324/9780203799574-12/heterotopias-experience-porous-urban-space-stavrides>.
- Steven Holl Architects. (2016). *The Porous School*. Steven Holl Architects: Visual Arts Building, University of Iowa, Retrieved November 27, 2022, from <https://e-zeppelin.ro/en/the-porous-school-steven-holl-architects-visual-arts-building-university-of-iowa/>.
- Thierstein, A. (2018). The Connected and Multiscalar City: Porosity in the Twenty-first Century. In S. Wolfrum (Ed.), *Porous City: From Metaphor to Urban Agenda* (pp. 222–225). Birkhäuser. <https://doi.org/10.1515/9783035615784-048>
- Uchiyama, Y., Blanco, E., & Kohsaka, R. (2020). Application of biomimetics to architectural and urban design: a review across scales. *Sustainability*, 12(23), 9813.
- Ursprung, P. (2018). Holes in the Future City: Java's Volcanoes. In S. Wolfrum (Ed.), *Porous City: From Metaphor to Urban Agenda* (pp. 210–217). Birkhäuser. <https://doi.org/10.1515/9783035615784-046>
- Wolfrum, S. (2018a). Porosity—Porous City. In S. Wolfrum (Ed.), *Porous City: From Metaphor to Urban Agenda* (pp. 17–19). Birkhäuser. <https://doi.org/10.1515/9783035615784-002>
- Wolfrum, S. (2018b). Porous City—From Metaphor to Urban Agenda. In S. Wolfrum (Ed.), *Porous City: From Metaphor to Urban Agenda* (pp. 9–14). Birkhäuser. <https://doi.org/10.1515/9783035615784-001>
- Xu, W. G., & Li, N. (2018). *Digital Diagrams from BIO-Form for Architectural Design*. China Construction Industry Press.
- Yuan, C., & Ng, E. (2012). Building porosity for better urban ventilation in high-density cities—A computational parametric study. *Building and Environment*, 50, 176–189. <https://doi.org/10.1016/j.buildenv.2011.10.023>
- Zöhrer, C. (2018). Exploring the Unforeseen—Porosity as a Concept. In S. Wolfrum (Ed.), *Porous City: From Metaphor to Urban Agenda* (pp. 58–59). Birkhäuser. <https://doi.org/10.1515/9783035615784-010>

## Publisher's Note

Springer Nature remains neutral with regard to jurisdictional claims in published maps and institutional affiliations.